Band-Gap Nonlinearity in Lead Chalcogenide (PbQ, Q = Te, Se, S) Alloys

AMINORROAYA YAMINI, Sima <http://orcid.org/0000-0002-2312-8272>, PATTERSON, Vaughan and SANTOS, Rafael

Published version

AMINORROAYA YAMINI, Sima, PATTERSON, Vaughan and SANTOS, Rafael (2017). Band-Gap Nonlinearity in Lead Chalcogenide (PbQ, Q = Te, Se, S) Alloys. ACS Omega, 2 (7), 3417-3423.

ACS OMEGA

Article

http://pubs.acs.org/journal/acsodf

Band-Gap Nonlinearity in Lead Chalcogenide (PbQ, Q = Te, Se, S) Alloys

Sima Aminorroaya Yamini,[†,*] Vaughan Patterson, and Rafael Santos

Australian Institute for Innovative Materials (AIIM), Innovation Campus, University of Wollongong, Squires Way, North Wollongong, NSW 2500, Australia

ABSTRACT: Narrow band-gap lead chalcogenides have been developed for several optical and electronic applications. However, band-gap energies of the ternary and quaternary alloys have received little attention compared with the parent binary phases. Here, we have fabricated single-phase ternary $(PbTe)_{1-x}(PbSe)_x$ and quaternary $(PbTe)_{0.9-y}(PbSe)_{0.1}(PbS)_y$ and $(PbTe)_{0.65-z}(PbSe)_{0.35}(PbS)_z$ alloys and shown that although lattice parameters follow Vegard's law as a function of composition, the band-gap energies exhibit a substantial bowing effect. The ternary $(PbTe)_{1-x}(PbSe)_x$ system features a smaller bowing parameter predominantly due to the difference in electronegativity between Se and Te, whereas the larger bowing parameters in quaternary alloys are generated from a larger crystal lattice mismatch and larger miscibility gap. These findings can lead to further advances in tuning the band-gap and lattice parameters for optical and electronic applications of lead chalcogenides.

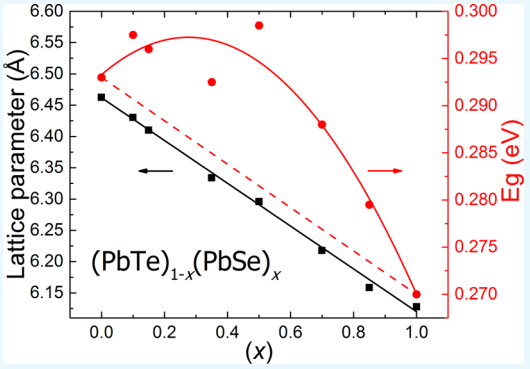

INTRODUCTION

Lead chalcogenides (PbQ, Q = Te, Se, S) are unique compared with other semiconductors due to their interesting electronic and transport properties, such as narrow band gaps, low resistivities, large carrier mobilities, and positive temperature coefficients, showing an increase in the energy of band gap with temperature.[1−3] These optical and electronic properties have led to the development of lead chalcogenides for several applications, including infrared lasers and detectors,[4] thermophotovoltaics,[5] infrared optoelectronic devices,[6] photovoltaics,[7] and thermoelectrics.[8−11]

The optical and thermoelectric properties of lead chalcogenides have been shown to vary significantly with alloying.[11−15] Despite significant recognition of band engineering in lead chalcogenide alloys,[11,16,17] the band-gap energies of ternary and quaternary lead chalcogenides have received little attention in contrast to the parent binary phases of PbTe, PbSe, and PbS. Conventional semiconductor physics wisdom suggests that "band-gap bowing" is a common effect in semiconductor alloy systems[12,18−21] and that it is likely present in lead chalcogenide alloys as well. Regardless, many authors have overlooked this and assumed that lead chalcogenide alloy band gaps change linearly with composition, in a similar way to their lattice parameters.[8,14,22,23] This work aims to provide a better understanding of the band gap and bowing parameters for a wide range of lead chalcogenide alloys, to provide fundamental information required to tune the energy gap for optoelectronic and electronic applications.

In this work, we have fabricated intrinsic polycrystalline single-phase bulk ternary and quaternary lead chalcogenide alloys and measured their room-temperature energy gaps. The ternary system of $(PbTe)_{1-x}(PbSe)_x$ was selected to determine the effect of PbSe content on the band-gap energy of PbTe. Whereas, quaternary samples of $(PbTe)_{0.9-y}(PbSe)_{0.1}(PbS)_y$ and $(PbTe)_{0.65-z}(PbSe)_{0.35}(PbS)_z$ were specially fabricated to elucidate the effects of PbS alloying on the band gap of ternary solid solution alloys of $(PbTe)_{0.9}(PbSe)_{0.1}$ and $(PbTe)_{0.65}(PbSe)_{0.35}$, respectively.

We show that although the lattice parameter variation of alloys with composition follows Vegard's law, the energy gaps exhibit nonlinearity. The measured room-temperature band gaps, as a function of composition, consistently differ from any linear projection and show a deviation, with a parabolic function (bowing). Bowing parameters have been determined for ternary and quaternary systems, and factors influencing the degree of bowing are described in detail.

RESULTS AND DISCUSSION

Extrinsically doped semiconductors show high charge-carrier concentrations that increase the measured optical band-gap energy values due to the Burstein−Moss shift.[24] Therefore, all samples in the current study were undoped. The room-temperature electrical resistivity of sintered samples was measured to assure negligible effect of intrinsic doping. Extrinsically doped n-type and p-type lead chalcogenides show room-temperature resistivity values below 1 mΩ cm, whereas the current study samples show resistivities between 6 and 90 mΩ cm.[25] Nevertheless, the optical band gaps measured for n-type PbTe samples show a noticeable increase in band-

Received: April 30, 2017
Accepted: July 3, 2017
Published: July 11, 2017

DOI: 10.1021/acsomega.7b00539
ACS Omega 2017, 2, 3417−3423

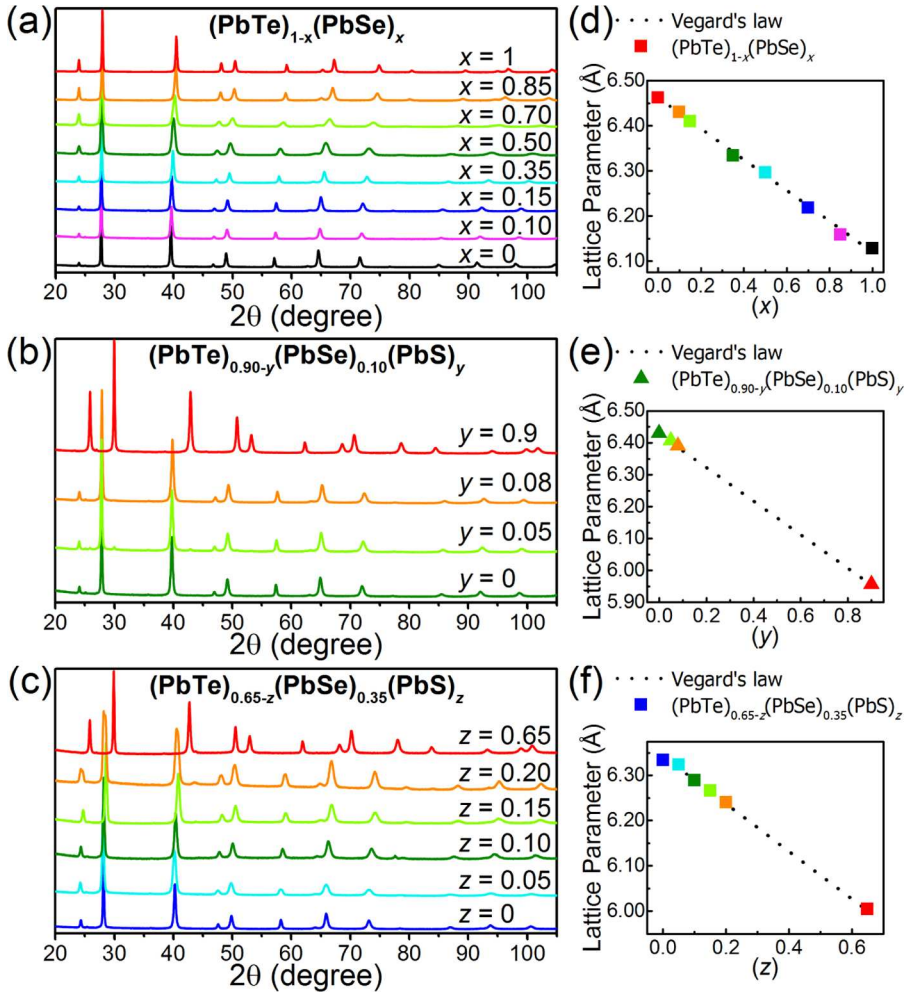

Figure 1. Powder XRD patterns of (a) ternary $(PbTe)_{(1-x)}(PbSe)_x$ (x = 0, 0.10, 0.15, 0.35, 0.50, 0.70, 0.85, and 1.0), (b) quaternary $(PbTe)_{0.9-y}(PbSe)_{0.1}(PbS)_y$ (y = 0, 0.05, 0.08, and 0.9), and (c) quaternary $(PbTe)_{0.65-z}(PbSe)_{0.35}(PbS)_z$ (z = 0, 0.05, 0.10, 0.15, 0.20, and 0.65) alloys. Lattice parameters of (d) ternary $(PbTe)_{(1-x)}(PbSe)_x$ (x = 0, 0.10, 0.15, 0.35, 0.50, 0.70, 0.85, and 1.0), (e) quaternary $(PbTe)_{0.9-y}(PbSe)_{0.1}(PbS)_y$ (y = 0, 0.05, 0.08, and 0.9), and (f) quaternary $(PbTe)_{0.65-z}(PbSe)_{0.35}(PbS)_z$ (z = 0, 0.05, 0.10, 0.15, 0.20, and 0.65) alloys as a function of composition.

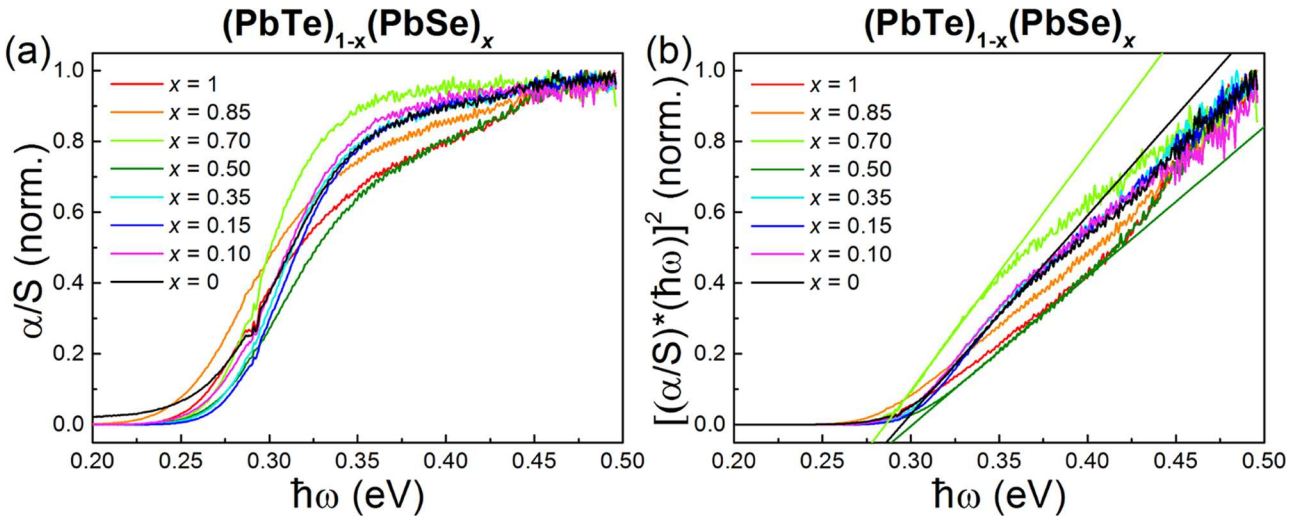

Figure 2. (a) Normalized Kubelka–Munk transformations for the ternary $(PbTe)_{(1-x)}(PbSe)_x$ (x = 0, 0.10, 0.15, 0.35, 0.50, 0.70, 0.85, and 1.0) system from raw data obtained using diffuse reflectance infrared Fourier transform spectroscopy (DRIFTS). (b) Normalized Kubelka–Munk function for the ternary $(PbTe)_{(1-x)}(PbSe)_x$ (x = 0, 0.10, 0.15, 0.35, 0.50, 0.70, 0.85, and 1.0) system for absorption coefficient fit along with a few linear extrapolations to obtain the direct band gap by the Tauc method.

DOI: 10.1021/acsomega.7b00539
ACS Omega 2017, 2, 3417–3423

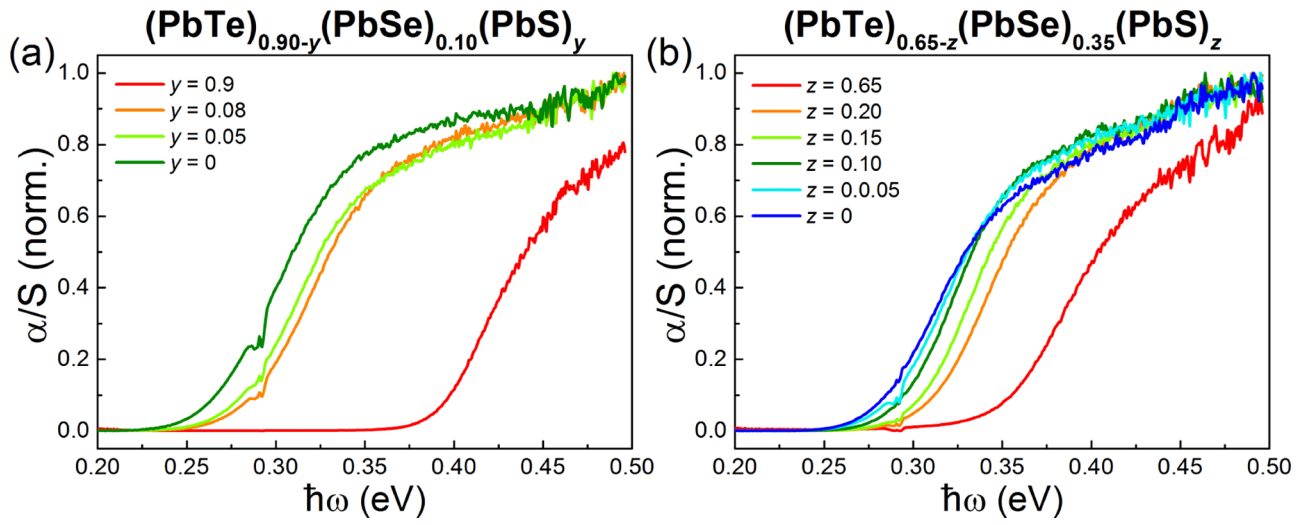

Figure 3. Normalized Kubelka–Munk transformations for quaternary alloys of (a) $(PbTe)_{0.9-y}(PbSe)_{0.1}(PbS)_y$ (y = 0, 0.05, 0.08, and 0.9) and (b) $(PbTe)_{0.65-z}(PbSe)_{0.35}(PbS)_z$ (z = 0, 0.05, 0.10, 0.15, 0.20, and 0.65) for application of the Tauc method for determining direct band gaps.

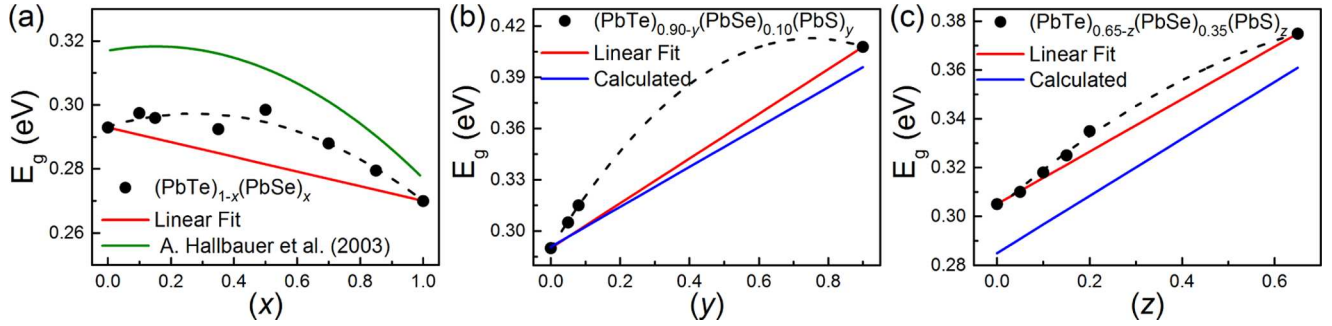

Figure 4. Direct band-gap energies for (a) the ternary $(PbTe)_{(1-x)}(PbSe)_x$ (x = 0, 0.10, 0.15, 0.35, 0.50, 0.70, 0.85, and 1.0) system as a function of the PbSe content, compared to those of films grown by the molecular beam epitaxy method;[6] (b) the quaternary $(PbTe)_{0.9-y}(PbSe)_{0.1}(PbS)_y$ system and (c) the $(PbTe)_{0.65-z}(PbSe)_{0.35}(PbS)_z$ system as functions of PbS concentration.

gap energy due to Burstein–Moss shift for heavily doped samples with carrier concentrations above 10^{19} cm^{-3}, corresponding to electrical resistivities below ~0.5 mΩ cm.[24] This indicates that band-gap energies of current study samples are hardly affected by the Burstein–Moss effect.

A single-phase sample is also vital in obtaining an accurate band-gap measurement, as it has been shown that precipitation of secondary phases can incorrectly increase the measured optical energy gap for semiconductors.[26] The solubility of PbS in PbTe is very limited due to a large miscibility gap that exists between these binary compounds where the phase separation occurs[27] and results in the precipitation of PbS within the PbTe matrix at concentrations as low as 4 atom % PbS.[28] Therefore, the selected compositions for quaternary systems lie outside the miscibility gaps wherein only single-phase alloys can be obtained. The presence of PbSe in quaternary compounds $(PbTe)_{0.9-y}(PbSe)_{0.1}(PbS)_y$ has been shown to increase PbS solubility in the ternary alloy $(PbTe)_{0.9}(PbSe)_{0.1}$.[9,10]

Crystal Structure. X-ray diffraction (XRD) patterns of $(PbTe)_{(1-x)}(PbSe)_x$ (x = 0, 0.10, 0.15, 0.35, 0.50, 0.70, 0.85, and 1.0), $(PbTe)_{0.9-y}(PbSe)_{0.1}(PbS)_y$ (y = 0, 0.05, 0.08, and 0.9), and $(PbTe)_{0.65-z}(PbSe)_{0.35}(PbS)_z$ (z = 0, 0.05, 0.10, 0.15, 0.20, and 0.65) samples are shown in Figure 1a–c, respectively. All patterns show the single-phase NaCl-type face-centered cubic structure. Figure 2 shows that diffraction peaks are progressively shifted to a higher angle by increasing PbSe and PbS concentrations. The lattice parameter of the PbTe (a = 6.46 Å) phase is larger than that of PbSe (a = 6.13 Å) and PbS (a = 5.93 Å). Rietveld refinement was employed to accurately determine lattice parameters of all samples by extrapolating from high angle diffraction peaks. The results (Figure 1d–f) show that the lattice parameters of the alloys change linearly with composition and follow Vegard's Law, indicating solid solution phases for all systems.

Optical Band-Gap Energy. The room-temperature absorption coefficient was calculated using the Kubelka–Munk function (α/S), where α is the absorption and S the scattering coefficient, respectively. Normalized spectra are shown in Figure 2a for the ternary $(PbTe)_{(1-x)}(PbSe)_x$ (x = 0, 0.10, 0.15, 0.35, 0.50, 0.70, 0.85, and 1.0) system. Optical band-gap energies are determined by applying the Tauc method, where $(\alpha h\omega)^n$ is extrapolated to zero as a function of the incoming photon energy ($h\omega$) for direct gap semiconductors (n = 2)[24] (Figure 2b for the $(PbTe)_{(1-x)}(PbSe)_x$ system).

Band-gap energies of $(PbTe)_{0.9-y}(PbSe)_{0.1}(PbS)_y$ (y = 0, 0.05, 0.08, and 0.9) and $(PbTe)_{0.65-z}(PbSe)_{0.35}(PbS)_z$ (z = 0, 0.05, 0.10, 0.15, 0.20, and 0.65) samples were calculated from the normalized Kubelka–Munk graph shown in Figure 3a,b, respectively. The shift in energy of the band gaps to higher values with PbS content is evident in the quaternary samples compared to that in the ternary system. The band-gap energy of

DOI: 10.1021/acsomega.7b00539
ACS Omega 2017, 2, 3417–3423

Table 1. Summary of Physical Properties Affecting the Bowing Parameter of Lead Chalcogenide Alloys

compound	anion radius (Å)[30]	lattice constant (Å)[1]	electronegativity of anions[31]	valence electron potential ($-eV$)	band gap (eV)[1]
PbS	1.84	5.94	2.58	160	0.41
PbSe	1.98	6.12	2.55	120	0.27
PbTe	2.21	6.50	2.10	59	0.29

PbS (0.41 eV) is much higher than that of PbSe (0.27 eV) and PbTe (0.29 eV) and hence there is a large difference in the energy gap between the PbS-free samples $(PbTe)_{0.9}(PbSe)_{0.1}$ and $(PbTe)_{0.65}(PbSe)_{0.35}$ and the PbTe-free samples $(PbSe)_{0.1}(PbS)_{0.9}$ and $(PbSe)_{0.35}(PbS)_{0.65}$, resulting in a larger energy range for the measurements to spread across.

Figure 4a illustrates nonlinear variation of the optical band gap of ternary $(PbTe)_{(1-x)}(PbSe)_x$ alloys with composition. Although the differences in the measured band gaps from linear assumption values are small, the adopted measurement technique DRIFTS has been shown to be reliable in quantifying changes in the band gap, with high resolution of ±0.004 eV.[24] It is evident that the band gaps of $(PbTe)_{(1-x)}(PbSe)_x$ alloys vary in a parabolic contour with composition rather than in a linear relationship. This deviation is due to a phenomenon known as the bowing effect. This effect has been previously observed in $(PbTe)_{(1-x)}(PbSe)_x$ alloys grown on the (111) BaF_2 substrate by the molecular beam epitaxy method[6] (Figure 4a). Although both studies show a bowing effect, the measured energy gaps are different. This might have originated from fabrication methods. The molecular beam epitaxy technique might have introduced point defects in the structure, resulting in higher carrier concentration, which is shown to increase the optical band gap due to the Burstein−Moss effect.[25]

Figure 4b,c shows the calculated linear assumption and measured variation of the direct band-gap energy with respect to the PbS content for quaternary systems of $(PbTe)_{0.9-y}(PbSe)_{0.1}(PbS)_y$ and $(PbTe)_{0.65-z}(PbSe)_{0.35}(PbS)_z$, respectively. The calculated curve is a linear prediction of the band gap, using the band-gap energy measured for pure binary phases of PbTe, PbSe, and PbS. The linear assumption lines in Figure 4b,c are the predicted variation in the energy of the band gaps with composition between the ternary alloys of PbS-free $(PbTe)_{0.9}(PbSe)_{0.1}$ and $(PbTe)_{0.65}(PbSe)_{0.35}$ and PbTe-free samples of $(PbSe)_{0.1}(PbS)_{0.9}$ and $(PbSe)_{0.35}(PbS)_{0.65}$. The curves in Figure 4b,c fit the parabolic equation for the measured energies of the band gaps. The experimental data in Figure 4c deviate slightly from the linear relationship, although the calculated curves for $(PbTe)_{0.9-y}(PbSe)_{0.1}(PbS)_y$ compounds show band gaps much smaller than with the linear assumption and experimental data due to the smaller band-gap values obtained for binary PbSe, PbTe, and PbS. It is worth noting that experimental band-gap energies measured for these binary compounds are equal to values extracted from the literature (Table 1). The composition gaps in the experimental data in Figure 4a,b exhibit a phase separation region, wherein the PbS-rich phase precipitates within the PbTe-rich matrix.[10,29]

The nonlinear nature of the variation of the optical band gap with composition is not uncommon and has been observed in a number of classical semiconductor systems, such as Si−Ge,[32] InGaN, AlGaN, AlInN,[18] and CdSe-CdTe.[33] The bowing parameter in semiconductors is described by a parabolic polynomial[12]

$$E_{g,AB} = xE_{g,A} + (1 - x)E_{g,B} - bx(1 - x) \quad (1)$$

where $E_{g,A}$ and $E_{g,B}$ are intrinsic energy gaps of the initial semiconductors A and B and x is the phase ratio of A that is used to calculate the energy gap of the alloy ($E_{g,AB}$). The degree to which the curve deviates from the linear fit is described by the bowing parameter b.[34]

Bowing parameters calculated for ternary and quaternary systems are summarized in Table 2. The negative sign of bowing parameters is due to the inverted nature of the parabola for these systems.[35] It is worth noting that the bowing parameter for the $(PbTe)_{0.9-y}(PbSe)_{0.1}(PbS)_y$ system has been obtained by fitting limited experimental data, which can contribute to a larger error value. Nevertheless, the absolute value of the bowing parameter (b) for the quaternary $(PbTe)_{0.65-z}(PbSe)_{0.35}(PbS)_z$ system (−0.08326 eV) is much smaller than that for the quaternary $(PbTe)_{0.9-y}(PbSe)_{0.1}(PbS)_y$ system (−0.21813 eV), larger than that (−0.052 eV) for the ternary $(PbTe)_{(1-x)}(PbS)_x$ system, and similar to that of the ternary $(PbSe)_{(1-x)}(PbS)_x$ system (−0.190 eV).[12] There are several factors that affect the bowing parameter of solid solution materials, including ionicity and crystal structure mismatch, solubility, electron potential, and electronegativity.[8,12,33,36]

Table 2. Bowing Parameter (b) Calculated for Band-Gap Energy of Ternary and Quaternary Systems

system	bowing parameter (eV)
$(PbTe)_{(1-x)}(PbSe)_x$	−(0.052 ± 0.011)
$(PbTe)_{0.9-y}(PbSe)_{0.1}(PbS)_y$	−(0.21813 ± 0.01561)
$(PbTe)_{0.65-z}(PbSe)_{0.35}(PbS)_z$	−(0.08326 ± 0.02352)
$(PbSe)_{(1-x)}(PbS)_x$[12]	−(0.190 ± 0.045)

Atomic Size and Ionicity. The atomic size and ionicity mismatch of the atoms have been shown to be the main cause for bowing of band gaps in solid solution semiconductor alloys.[20,32,34] In systems such as (Zn, Mg, Be)O,[34] $BaTiO_3$−$CaTiO_3$, $BaTiO_3$−$BaZrO_3$, $SrTiO_3$−$BaZrO_3$,[32] and $Mg_xZn_{1-x}Se$,[20] there are large variations in the atomic size and ionicity of participant atoms, which are believed to cause the band-gap bowing.

Lattice parameters of PbTe (6.50 Å) and PbSe (6.12 Å) are very similar but larger than those of PbS (5.94 Å). Concurrently, Se ions (1.98 Å) are slightly smaller than Te ions (2.21 Å), and both are larger than S ions (1.84 Å). All have valence 2^-. Therefore, it is unlikely that atomic size and ionicity play a significant role in the observed bowing of the band gap in ternary $(PbTe)_{(1-x)}(PbSe)_x$ and $(PbSe)_{(1-x)}(PbS)_x$ systems. On the other hand, replacing Te with S atoms in quaternary systems creates a slightly larger lattice mismatch that, in turn, increases the bowing parameter.[36]

Electronegativity. The electronegativity of individual anions bonded to cations has also been identified as a major factor determining the degree to which band-gap bowing occurs in alloys.[33] The electronegativity effect is used to measure an atom's ability to draw electrons from surrounding atoms toward it. It is determined by the atomic number and how far the outer electrons lie from the inner nucleus. The Pauling scale is the

DOI: 10.1021/acsomega.7b00539
ACS Omega 2017, 2, 3417−3423

most frequently used method to compare electronegativities, in which fluorine is given the highest value of 4.0, and this value decreases down through all elements to cesium and francium at 0.7.[31]

Electronegative values of Te, Se, and S atoms are 2.10, 2.55, and 2.58, respectively, according to the Pauling scale. The band-gap bowing in the ternary $(PbTe)_{(1-x)}(PbS)_x$ system might be attributed to the larger electronegativity of Se ions compared to that of Te ions (2.55 > 2.10). It is unlikely, however, that replacing Te ions with S ions with slightly larger electronegativity (2.58 > 2.55) in quaternary systems could cause bowing in the energy gaps.

Valence Electron Potential. Similar to electronegativity, conflicting valence electron potentials of individual atoms in a specific system have also been identified to play a significant role in the band-gap bowing of alloys. This valence electron potential is a quantitative indication of the reactivity of individual atoms and can be calculated using the equation[37]

$$-eV = \frac{kn}{r} \tag{2}$$

where $-eV$ is the valence electron potential, n is the number of valence electrons, r is the ionic radius (Å), and k is the proportionality factor used to convert angstrom (Å) into centimeter (cm) and transform the force of valence electrons into electron volt (eV).

The valence electron potential of S (160 eV) is higher than that of Se (120 eV) and is much higher than that of Te (59 eV), suggesting an increase in the core potential fluctuation and increased deviation from the symmetric alloy behavior.[35] Therefore, one would expect that quaternary systems show a larger bowing parameter than that of ternary compounds.

Solubility. The solubility of two compounds is directly linked to the magnitude of bowing in the band gaps of their alloys. Solubility is a direct reflection of atomic size, ionicity, and electronegativity.[38] Alloys that contain large regions where phase separation occurs tend to have larger bowing parameters than those of alloys with minimal or no miscibility gaps.[33,35]

It is evident from the pseudobinary phase diagram of PbSe–PbTe that the miscibility gap only occurs at temperatures below 170 K for $(PbTe)_{(1-x)}(PbSe)_x$ alloys.[39] Hence, the solubility factor has minimal influence on the band-gap bowing of the $(PbTe)_{(1-x)}(PbSe)_x$ system, although it might result in bowing of band gap for $(PbTe)_{0.9-y}(PbSe)_{0.1}(PbS)_y$ and $(PbTe)_{0.65-z}(PbSe)_{0.35}(PbS)_z$ systems, as their alloys have a sizeable miscibility gap.[29] The size of the miscibility gap for the $(PbTe)_{0.65-z}(PbSe)_{0.35}(PbS)_z$ system is much smaller than that of the $(PbTe)_{0.9-y}(PbSe)_{0.1}(PbS)_y$ system.[29] Therefore, one would expect to observe a larger bowing parameter for the $(PbTe)_{0.9-y}(PbSe)_{0.1}(PbS)_y$ system. Both quaternary systems show larger bowing parameters than those of ternary $(PbTe)_{1-x}(PbSe)_x$ alloys, with complete solubility over the whole composition range.

The solubility, atomic size, and ionicity factors suggest minimal band-gap bowing for ternary $(PbTe)_{(1-x)}(PbSe)_x$ and $(PbSe)_{(1-x)}(PbS)_x$ systems, whereas, the electron potential and electronegativity predict bowing in the energy of band gaps in the ternary $(PbTe)_{(1-x)}(PbSe)_x$ system. It is worth noting that the band gap for ternary $(PbSe)_{(1-x)}(PbS)_x$ alloys was determined for nanocrystals, suggesting that the bowing is influenced by quantum confinement and changes of the quantum dot size.[12] A linear relationship of band-gap energy with composition is expected for bulk $(PbSe)_{(1-x)}(PbS)_x$ alloys. On the other hand, the atomic size, electronegativity, and solubility that result in spinodal decomposition (below 1050 K) in the PbTe–PbS system appear to be likely factors behind the band-gap bowing of quaternary systems.

A potential reason for the reduced bowing parameter in the $(PbTe)_{0.65-z}(PbSe)_{0.35}(PbS)_z$ system compared to that of the $(PbTe)_{0.9-y}(PbSe)_{0.1}(PbS)_y$ system is the smaller miscibility gap that exists between the $(PbTe)_{0.65}(PbSe)_{0.35}$ and $(PbSe)_{0.35}(PbS)_{0.65}$ phases in the $(PbTe)_{0.65-z}(PbSe)_{0.35}(PbS)_z$ system compared to that between $(PbTe)_{0.9}(PbSe)_{0.1}$ and $(PbSe)_{0.1}(PbS)_{0.9}$ in the $(PbTe)_{0.9-y}(PbSe)_{0.1}(PbS)_y$ system.

CONCLUSIONS

The unique physical properties of Pb chalcogenides have led to their development for several optical and electronic applications, wherein the tuned band-gap energy can tailor electronic transport properties. Herein, intrinsic polycrystalline samples of ternary and quaternary Pb chalcogenide alloys were fabricated and their optical band-gap energies and lattice parameters were measured as a function of composition. Although lattice parameters of these alloys follow Vegard's equation, the band-gap energies exhibit nonlinear relationships with compositions. We have determined the bowing parameters for these systems.

The ternary $(PbTe)_{1-x}(PbSe)_x$ system featured a small amount of band-gap bowing, predominantly due to the difference in electronegativity between Se and Te. Bowing parameters for the quaternary $(PbTe)_{0.9-y}(PbSe)_{0.1}(PbS)_y$ system are larger than those for $(PbTe)_{0.65-z}(PbSe)_{0.35}(PbS)_z$ due to the larger crystal lattice mismatch and miscibility gap. This opens up promising perspectives for tuning the band-gap energy and lattice parameters of Pb chalcogenide alloys for optical and electronic applications.

METHODS

Sample Fabrication. Intrinsic polycrystalline samples of PbS, PbSe, and PbTe were prepared by mixing stoichiometric ratios of high purity Pb (99.999%), Se (99.999%), and dried S (99.99%) in vacuum-sealed quartz ampoules. These were reacted at 1373 K to produce high purity PbS, PbSe, and PbTe. The final polycrystalline samples of ternary and quaternary compounds of $(PbTe)_{1-x}(PbSe)_x$ (x = 0, 0.15, 0.35, 0.50, 0.70, 0.85, and 1), $(PbTe)_{0.9-y}(PbSe)_{0.1}(PbS)_y$ (y = 0, 0.05, 0.08, and 1), and $(PbTe)_{0.65-z}(PbSe)_{0.35}(PbS)_z$ (z = 0, 0.05, 0.10, 0.15, 0.20, and 1) were synthesized by mixing stoichiometric quantities of high purity PbS, PbSe, Pb, and Te. The mixtures were sealed in carbon-coated quartz tubes under vacuum, reacted at 1373 K for 10 h, and then cooled to room temperature in the furnace. The resulting ingots were hand-ground to powder in an agate mortar and used to measure the energy of band gaps.

XRD Analysis. The crystallographic structure of samples was characterized by XRD using a GBC Scientific X-ray diffractometer with Cu Kα radiation (λ = 1.544 Å, 40 kV, 30 mA). To measure phase ratios and calculate lattice parameters, XRD patterns were refined using the Rietveld analysis.

Infrared Optical Properties. Room-temperature diffuse reflectance spectra of finely ground powders were recorded using a Shimadzu IRPrestige-21 Fourier Transform Infrared (FTIR) Spectrophotometer equipped with diffuse reflectance. The spectra were monitored in the mid-IR region (6000–400 cm^{-1}), which were then converted to electron volts (eV) using

DOI: 10.1021/acsomega.7b00539
ACS Omega 2017, 2, 3417–3423

Planck's law. Absorption data (α/S) were calculated from reflectance data via the Kubelka–Munk transformation. Optical energy gaps were extracted using the Tauc method.[40]

AUTHOR INFORMATION

Corresponding Author

*E-mail: sima@uow.edu.au.

ORCID

Sima Aminorroaya Yamini: 0000-0002-2312-8272

Present Address

†Department of Engineering and Mathematics, Sheffield Hallam University, Sheffield S1 1WB, U.K. (S.A.Y.).

Notes

The authors declare no competing financial interest.

ACKNOWLEDGMENTS

This research has been conducted with the support of an Australian Research Council Discovery Early Career Award (DE130100310) and an Australian Government Research Training Program Scholarship. The authors would like to acknowledge Dr. Zachary Gibbs for his discussions and expert advice.

REFERENCES

(1) Ravich, Y. I.; Efimova, B. A.; Smirnov, I. A. Semiconducting Lead Chalcogenides. In *Monographs in Semiconductor Physics*; Stil'bans, L. S., Ed.; Plenum Press: New York, 1970.

(2) Cowley, R. A. On the theory of ferroelectricity and anharmonic effects in crystals. *Philos. Mag.* **1965**, *11*, 673–706.

(3) Gibbs, Z. M.; Kim, H.; Wang, H.; White, R. L.; Drymiotis, F.; Kaviany, M.; Jeffrey Snyder, G. Temperature dependent band gap in PbX (X = S, Se, Te). *Appl. Phys. Lett.* **2013**, *103*, No. 262109.

(4) Zogg, H.; Ishida, A. IV-VI (Lead Chalcogenide) Infrared Sensors and Lasers. In *Infrared Detectors and Emitters: Materials and Devices*; Capper, P., Elliott, C. T., Eds.; Springer US: Boston, MA, 2001; pp 43–75.

(5) Chaudhuri, T. K. A solar thermophotovoltaic converter using PbS photovoltaic cells. *Int. J. Energy Res.* **1992**, *16*, 481–487.

(6) Hallbauer, A.; Schwarzl, T.; Lechner, R. T.; Springholz, G. In *Molecular Beam Epitaxy of PbSe1-xTex for Strain Engineering in IV-VI Semiconductor Heterostructures*, Proceedings of GMe Forum; TU Wien, 2003.

(7) Semonin, O. E.; Luther, J. M.; Beard, M. C. Quantum dots for next-generation photovoltaics. *Mater. Today* **2012**, *15*, 508–515.

(8) Pei, Y.; Shi, X.; LaLonde, A.; Wang, H.; Chen, L.; Snyder, G. J. Convergence of electronic bands for high performance bulk thermoelectrics. *Nature* **2011**, *473*, 66–69.

(9) Aminorroaya Yamini, S.; Mitchell, D. R. G.; Gibbs, Z. M.; Santos, R.; Patterson, V.; Li, S.; Pei, Y. Z.; Dou, S. X.; Snyder, G. J. Heterogeneous distribution of sodium for high thermoelectric performance of p-type multiphase lead-chalcogenides. *Adv. Energy Mater.* **2015**, *5*, No. 1501047.

(10) Aminorroaya Yamini, S.; Wang, H.; Gibbs, Z.; Pei, Y.; Mitchell, D. R. G.; Dou, S. X.; Snyder, G. J. Thermoelectric performance of Tellurium-reduced quaternary p-type lead-chalcogenide composites. *Acta Mater.* **2014**, *80*, 365–372.

(11) Aminorroaya Yamini, S.; Wang, H.; Gibbs, Z.; Pei, Y.; Dou, S. X.; Snyder, G. J. Chemical composition tuning in quaternary p-type Pb-chalcogenides - A promising strategy for enhanced thermoelectric performance. *Phys. Chem. Chem. Phys.* **2014**, *16*, 1835–1840.

(12) Akhtar, J.; Afzaal, M.; Banski, M.; Podhorodecki, A.; Syperek, M.; Misiewicz, J.; Bangert, U.; Hardman, S. J. O.; Graham, D. M.; Flavell, W. R.; Binks, D. J.; Gardonio, S.; O'Brien, P. Controlled Synthesis of Tuned Bandgap Nanodimensional Alloys of PbS_xSe_{1-x}. *J. Am. Chem. Soc.* **2011**, *133*, 5602–5609.

(13) LaLonde, A. D.; Pei, Y.; Snyder, G. J. Reevaluation of PbTe1-xIx as high performance n-type thermoelectric material. *Energy Environ. Sci.* **2011**, *4*, 2090–2096.

(14) Korkosz, R. J.; Chasapis, T. C.; Lo, S.-h.; Doak, J. W.; Kim, Y. J.; Wu, C.-I.; Hatzikraniotis, E.; Hogan, T. P.; Seidman, D. N.; Wolverton, C.; Dravid, V. P.; Kanatzidis, M. G. High ZT in p-Type $(PbTe)_{1-2x}(PbSe)_x(PbS)_x$ Thermoelectric Materials. *J. Am. Chem. Soc.* **2014**, *136*, 3225–3237.

(15) Aminorroaya Yamini, S.; Wang, H.; Ginting, D.; Mitchell, D. R. G.; Dou, S. X.; Snyder, G. J. Thermoelectric performance of *n*-type $PbSe_{0.1}S_{0.15}Te_{0.75}$ composites. *ACS Appl. Mater. Interfaces* **2014**, *6*, 11476–11483.

(16) Pei, Y.; Wang, H.; Snyder, G. J. Band Engineering of Thermoelectric Materials. *Adv. Mater.* **2012**, *24*, 6125.

(17) Zhang, Q.; Cao, F.; Liu, W.; Lukas, K.; Yu, B.; Chen, S.; Opeil, C.; Broido, D.; Chen, G.; Ren, Z. Heavy Doping and Band Engineering by Potassium to Improve the Thermoelectric Figure of Merit in p-Type PbTe, PbSe, and $PbTe_{1-y}Se_y$. *J. Am. Chem. Soc.* **2012**, *134*, 10031–10038.

(18) Berrah, S.; Boukortt, A.; Abid, H. The composition effect on the bowing parameter in the cubic InGaN, AlGaN and AlInN alloys. *Semicond. Phys., Quantum Electron. Optoelectron.* **2008**, *11*, 59–62.

(19) Ferry, D. K. Semiconductors, Bonds and Bands. In *IOP Expanding Physics*; IOP Publishing: Bristol, U.K., 2013.

(20) Charifi, Z.; Baaziz, H.; Bouarissa, N. Energy band gaps of $Mg_xZn_{1-x}Se$: Violation of Vegard's law. *Int. J. Mod. Phys. B* **2004**, *18*, 137–142.

(21) Wei, S.-H.; Zunger, A. Electronic and structural anomalies in lead chalcogenides. *Phys. Rev. B* **1997**, *55*, 13605–13610.

(22) Dornhaus, R.; Nimtz, G.; Schlicht, B. Narrow-Gap Semiconductors. In *Springer Tracts in Modern Physics*; Springer: Berlin, 1983.

(23) Fano, V. Lead Telluride and Its Alloys. In *CRC Handbook of Thermoelectrics*; CRC Press, 1995.

(24) Gibbs, Z. M.; LaLonde, A.; Snyder, G. J. Optical band gap and the Burstein–Moss effect in iodine doped PbTe using diffuse reflectance infrared Fourier transform spectroscopy. *New J. Phys.* **2013**, *15*, No. 075020.

(25) Patterson, V. *Band Gap Study of Lead Chalcogenide Alloys*; University of Wollongong: 2017.

(26) Ahn, S.; Jung, S.; Gwak, J.; Cho, A.; Shin, K.; Yoon, K.; Park, D.; Cheong, H.; Yun, J. H. Determination of band gap energy (Eg) of $Cu_2ZnSnSe_4$ thin films: On the discrepancies of reported band gap values. *Appl. Phys. Lett.* **2010**, *97*, No. 021905.

(27) Volykhov, A.; Yashina, L.; Shtanov, V. Phase relations in pseudobinary systems of germanium, tin, and lead chalcogenides. *Inorg. Mater.* **2006**, *42*, 596–604.

(28) Girard, S. N.; Schmidt-Rohr, K.; Chasapis, T. C.; Hatzikraniotis, E.; Njegic, B.; Levin, E. M.; Rawal, A.; Paraskevopoulos, K. M.; Kanatzidis, M. G. Analysis of Phase Separation in High Performance PbTe–PbS Thermoelectric Materials. *Adv. Funct. Mater.* **2013**, *23*, 747–757.

(29) Volykhov, A.; Yashina, L.; Shtanov, V. Phase equilibria in pseudoternary systems of IV–VI compounds. *Inorg. Mater.* **2010**, *46*, 464–471.

(30) Shannon, R. D. Revised effective ionic radii and systematic studies of interatomic distances in halides and chalcogenides. *Acta Crystallogr., Sect. A: Cryst. Phys., Diffr., Theor. Gen. Crystallogr.* **1976**, *32*, 751–767.

(31) Pauling, L. *The Chemical Bond: A Brief Introduction to Modern Structural Chemistry*; Cornell University Press, 1967.

(32) Lee, S.; Levi, R. D.; Qu, W.; Lee, C.; Randall, C. A. Band-gap nonlinearity in perovskite structured solid solutions. *J. Appl. Phys.* **2010**, *107*, No. 023523.

(33) Tit, N.; Obaidat, I. M.; Alawadhi, H. Origins of bandgap bowing in compound-semiconductor common-cation ternary alloys. *J. Phys.: Condens. Matter* **2009**, *21*, No. 075802.

DOI: 10.1021/acsomega.7b00539
ACS Omega 2017, 2, 3417–3423

(34) Shi, H.-L.; Duan, Y. Band-gap bowing and p-type doping of (Zn, Mg, Be)O wide-gapsemiconductor alloys: A first-principles study. *Eur. Phys. J. B* **2008**, *66*, 439−444.
(35) Rockett, A. *The Materials Science of Semiconductors*; Springer US: New York, 2010.
(36) Boukhris, N.; Meradji, H.; Ghemid, S.; Drablia, S.; Hassan, F. E. H. Ab initio study of the structural, electronic and thermodynamic properties of $PbSe_{1-x}$ S_x, $PbSe_{1-x}$ Te_x and PbS_{1-x} Te_x ternary alloys. *Phys. Scr.* **2011**, *83*, No. 065701.
(37) Phillips, J. C.; Kleinman, L. New method for calculating wave functions in crystals and molecules. *Phys. Rev.* **1959**, *116*, 287.
(38) Mizutani, U. *Hume-Rothery Rules for Structurally Complex Alloy Phases*; CRC Press, 2010.
(39) Doak, J. W.; Wolverton, C. Coherent and incoherent phase stabilities of thermoelectric rocksalt IV-VI semiconductor alloys. *Phys. Rev. B* **2012**, *86*, No. 144202.
(40) Tauc, J. Optical properties and electronic structure of amorphous Ge and Si. *Mater. Res. Bull.* **1968**, *3*, 37−46.

DOI: 10.1021/acsomega.7b00539
ACS Omega 2017, 2, 3417−3423